

Characterization and Attenuation of Sandwiched Deadband Problem Using Describing Function Analysis and Application to Electrohydraulic Systems Controlled by Closed-Center Valves

Song Liu

Bin Yao¹

Professor

e-mail: byao@purdue.edu

School of Mechanical Engineering,
Purdue University,
West Lafayette, IN 47907

Unlike input deadband, the sandwiched deadband between actuator and plant dynamics is very difficult to be explicitly compensated for due to the proceeding actuator dynamics whose effect may not be negligible. The paper presents a practical way to overcome the design conservativeness of existing methods in dealing with sandwiched deadband. Specifically, a describing function based nonlinear analysis method is proposed to characterize the effect of the sandwiched deadband on the stability and performance of the overall closed-loop system. The analysis results can be used to determine the highest closed-loop bandwidth that can be achieved without inducing residual limit cycles and instability. Optimal controller parameters can then be found to maximize the achievable closed-loop control performance. The technique is applied to an electrohydraulic system controlled by closed-center valves and a nonlinear feedback controller. Simulation results showed severe oscillations as the feedback control gains are increased to the predicted threshold values. Comparative experimental results also showed the effectiveness of the proposed method in reducing the conservativeness of traditional design and the improved closed-loop control performance in implementation. [DOI: 10.1115/1.3089557]

Keywords: deadband, describing function, electrohydraulics

1 Introduction

Sandwiched deadband systems have a nonlinear static deadband function between two dynamic components, usually the actuator dynamics and the plant dynamics, as shown in Fig. 1. The plant here refers to the system to be controlled, while the actuator refers to the physical device that accepts control signal and generates corresponding actions that can physically influence the plant response. If the actuator dynamics have sufficiently fast responses (i.e., sufficiently high bandwidth) when compared with the closed-loop dynamics, it can be safely neglected in the controller design and analysis. In such a case, the actuator can simply be considered as a static mapping or a gain in Fig. 1 and the sandwiched deadband essentially becomes an input deadband whose effect can be explicitly canceled or compensated with an inverse deadband function in the controller. The problem becomes very difficult to handle when the actuator dynamics are non-negligible.

Sandwiched deadbands are common nuisances that exist in many systems, such as the hydraulic arm controlled by overlapped closed-center proportional directional control (PDC) valves stud-

ied in this paper. The valve accepts the control signal and moves the spool to open/close the hydraulic circuitry to regulate the flow to the hydraulic cylinder that powers the hydraulic arm. For PDC valves of overlapped spool type, a deadband exists from the spool displacement to the valve flow that actually regulates motion of the hydraulic system. For such a system, the actuator dynamics refers to the valve or spool dynamics from the control input signal to the spool displacement, and the plant dynamics are from the valve flow to the hydraulic arm motion to be controlled, which include the mechanical arm dynamics and the hydraulic cylinder dynamics.

Several methods have been presented to deal with the problem of having non-negligible actuator dynamics. One is to use a feed-forward controller to boost the actuator dynamic response so that it would be sufficiently fast to be neglected [1], as shown in Fig. 2. Once the actuator dynamics are neglected, the deadband becomes an input deadband, which can be compensated by an inverse deadband function in the controller directly. However, the success of such a strategy depends on the accuracy of the actuator dynamic model. This method can only achieve some limited improvements in practice due to the unavoidable uncertainties in any physical systems.

Another way is to use local high gain feedback at the actuator level to attenuate the sandwiched deadband [2,3,1], as illustrated in Fig. 3. However, to apply this technique, the feedback of the actuator states or output is required. This may significantly increase the system cost or even be impossible for some systems. For example, to apply the feedback compensation to electrohy-

¹Corresponding author. Also a Kuang-piu Professor at the State Key Laboratory of Fluid Power Transmission and Control, Zhejiang University, Hangzhou, China.

Contributed by the Dynamic Systems, Measurement, and Control Division of ASME for publication in the JOURNAL OF DYNAMIC SYSTEMS, MEASUREMENT, AND CONTROL. Manuscript received April 4, 2005; final manuscript received December 31, 2008; published online March 19, 2009. Assoc. Editor: Noah Manning. Paper presented at the 2004 ASME International Mechanical Engineering Congress (IMECE2004), Anaheim, CA, November 13–19, 2004.

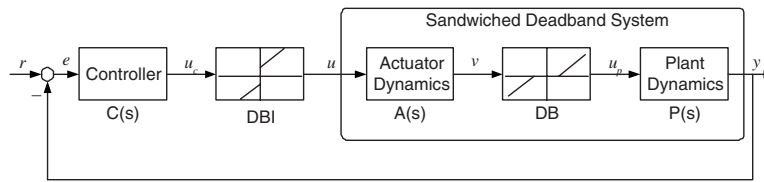


Fig. 1 Direct compensation of sandwiched deadband

hydraulic systems controlled by closed-center PDC valves, the feedback of valve-spool position is required. Although the spool position feedback is available in some valves, it is not a general valve configuration and would definitely increase the system cost. In addition, the improvement of local closed-loop bandwidth is limited by the sensor/feedback bandwidth and high frequency noise. For example, the spool position measurement in a PDC valve has significant noise content that prevents further significant improvement on the valve bandwidth achieved by the valve manufacturer [1,4].

Most of the existing designs to the control of sandwiched deadband system are to simply ignore the actuator dynamics and use an inverse deadband function to compensate for the deadband, as shown in Fig. 1. This solution is simple, easy to implement, and is used in a lot of applications such as in Ref. [5]. Such a deadband compensation usually results in a very conservative controller design because the closed-loop bandwidth has to be tuned very low to guarantee that the actuator dynamics can be safely neglected (e.g., the empirical rule of thumb that the closed-loop bandwidth has to be at least a decade below the actuator dynamics bandwidth). In reality, when the closed-loop bandwidth is increased to certain level, a limit cycle or instability could occur because the actuator dynamics makes the deadband compensation never perfect. A limit cycle is potentially very dangerous to systems with neglected vibration modes, because it may excite the vibration modes or even destabilize the system.

The describing function method is based on quasilinearization and replaces the nonlinear system under investigation with a system that is linear except for a dependence on the amplitude of the input [6]. Since it was proposed in 1947, the describing function method has been widely used to analyze nonlinear control problem when limit cycles may occur [7].

This paper focuses on reducing the conservativeness of the traditional direct deadband compensation designs to provide a practical solution to the sandwiched deadband control problem when actuator dynamics are not explicitly considered in the controller design stage. Specifically, though direct deadband compensation designs have been widely employed to deal with the sandwiched deadband control problem, no systematical way exists to guide the

selection of feedback controller parameters to optimize the achievable closed-loop system performance without exciting a limit cycle and instability. To overcome this problem, the describing function method will be used to systematically analyze and characterize the effect of sandwiched deadband on closed-loop system behavior. The analysis would give one a good idea about when a limit cycle would occur so that one can select the appropriate feedback controller gains to maximize the achievable closed-loop bandwidth without exciting limit cycles in implementation.

Closed-center valves are widely used in hydraulic industry for motion or velocity control due to the ability to hold position when the hydraulic power is turned off. Such ability is obtained through the use of overlapped spools, which block the internal leakages among various ports when the spool is at neutral position, as shown in Fig. 4. However, the use of overlapped spools also adds a deadband from the spool displacement to the actual opening of the valve ports (or valve port flows) to the system. It is obvious that this deadband is after the valve dynamics from the control input to the spool displacement and therefore is sandwiched by two dynamic blocks, the valve dynamics and the plant dynamics.

The paper uses the closed-center valve controlled electrohydraulic (EH) system as a case study to illustrate how to apply the proposed technique to a sandwiched deadband control problem to optimize the achievable closed-loop system performance in implementation. In particular, the swing motion of a robot arm actuated by a single-rod double-acting hydraulic cylinder, as detailed in Ref. [8], is investigated in detail.

2 Characterization of Sandwiched Deadband Systems Using Describing Function Analysis

A closed-loop system with sandwiched deadband $DB(\cdot)$ between the actuator dynamics $A(s)$ and the plant dynamics $P(s)$, and a linear feedback controller $C(s)$ along with a direct inverse deadband compensation $DBI(\cdot)$, shown in Fig. 1, is investigated in this section. The describing functions of the deadband and its inverse function are derived and used to characterize the closed-loop system performance.

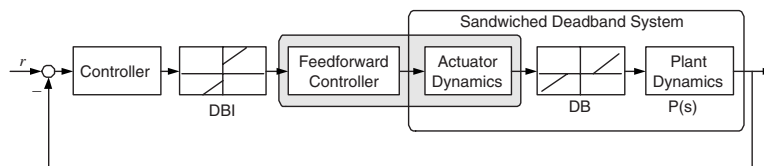


Fig. 2 Feed-forward control of sandwiched deadband

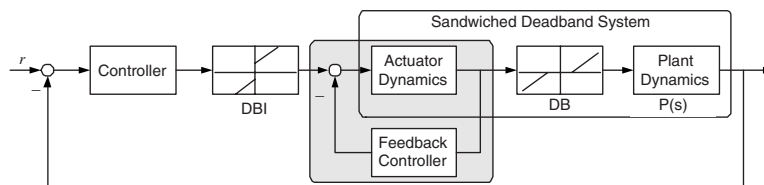


Fig. 3 Feedback control of sandwiched deadband

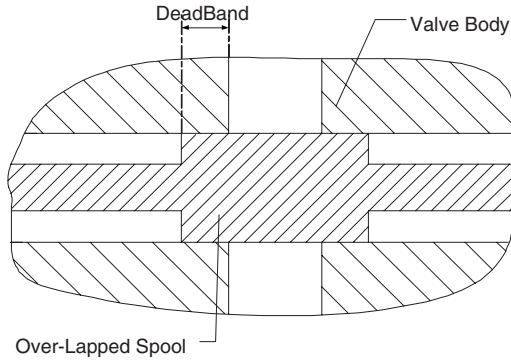


Fig. 4 Overlapped spool of a closed-center valve

2.1 Deadband and Inverse Deadband Functions. Consider a nonlinear function $f(y)$ under a sinusoidal input $y = a \sin(\omega t)$. One can use a gain $K(a)$, which is a function of the magnitude of the input sinusoidal signal, to approximate the nonlinear function. The mean square (MS) approximation error is

$$\bar{e}^2 = \frac{1}{2\pi} \int_0^{2\pi} [f(a \sin(\omega t)) - K(a)a \sin(\omega t)]^2 d(\omega t) \quad (1)$$

The solution of $K(a)$ to minimize the above MS error results in the describing function of the nonlinear function $f(\cdot)$ [9]

$$K(a) = \frac{1}{\pi a} \int_0^{2\pi} f(a \sin(\omega t)) \sin(\omega t) d(\omega t) \quad (2)$$

For simplicity, only symmetric deadband with slope equal to 1 is considered in this paper. Nonunity slope or asymmetric deadband can be worked out in the same way with minor modifications. Define the deadband and deadband inverse function as

$$\text{DB}(\cdot) = \begin{cases} -d, & \cdot > d \\ 0, & -d \leq \cdot \leq d \\ \cdot + d, & \cdot < -d \end{cases} \quad (3)$$

$$\text{DBI}(\cdot) = \begin{cases} \cdot + d, & \cdot > 0 \\ 0, & \cdot = 0 \\ \cdot - d, & \cdot < 0 \end{cases}$$

where d is the value of deadband. Substituting the $\text{DB}(\cdot)$ and $\text{DBI}(\cdot)$ into Eq. (2), one can obtain their describing functions as

$$K_{\text{DB}}(a) = \begin{cases} 0, & a < d \\ 1 - \frac{2d}{\pi a} \sqrt{1 - \frac{d^2}{a^2}} - \frac{2}{\pi} \sin^{-1} \frac{d}{a}, & a \geq d \end{cases} \quad (4)$$

$$K_{\text{DBI}}(a) = 1 + \frac{4d}{\pi a}$$

2.2 Characterization of Closed-Loop Systems. Deadband has a significant effect only when its input signal is around the deadzone of $[-d, d]$, which is normally very small. Therefore, without loss of generality, it is reasonable to assume $r=0$ in Fig. 1 (after the constant equilibrium components have been removed). We also only consider small amplitude limit cycles that may result from the deadband and its inverse as we are interested in looking at the upper bound on the highest closed-loop bandwidth, which can be achieved without inducing limit cycles. Since the limit cycle means a periodic signal in the closed-loop system, one can denote the signal right before the deadband inverse function

$\text{DBI}(\cdot)$ as $u_c = a \sin(\omega t)$ with a being the magnitude and ω representing the fundamental frequency of the limit cycle when only its fundamental frequency component is considered.

When a sinusoidal signal goes through an odd static function like the symmetric deadband considered in the paper, only its magnitude is changed, and its phase remains the same. Therefore, with the describing function approximation, the signal after the deadband inverse, denoted by u , would be

$$u(t) = K_{\text{DBI}}(a) \cdot a \sin(\omega t) \quad (5)$$

The control signal $u(t)$ then enters the actuator dynamics $A(s)$ and leaves it with changes in both magnitude and phase angle at the steady-state given by

$$v(t) = K_{\text{DBI}}(a) |A(j\omega)| \cdot a \sin(\omega t + \phi_A(j\omega)) \quad (6)$$

where $\phi_A(j\omega)$ is the phase angle of $A(j\omega)$. As the signal continues along the deadband function $\text{DB}(\cdot)$ and plant dynamics $P(s)$, the steady-state signals u_p and y are obtained as

$$u_p(t) = K_{\text{DB}}(K_{\text{DBI}}(a) |A(j\omega)| a) \cdot K_{\text{DBI}}(a) |A(j\omega)| \cdot a \sin(\omega t + \phi_A(j\omega)) \quad (7)$$

and

$$y = |P(j\omega)| K_{\text{DB}}(K_{\text{DBI}}(a) |A(j\omega)| a) \cdot K_{\text{DBI}}(a) |A(j\omega)| a \sin(\omega t + \phi_A(j\omega) + \phi_P(j\omega)) \quad (8)$$

where $\phi_P(j\omega)$ is the phase angle of $P(j\omega)$. Since $r=0$, $U_c(s) = -C(s)Y(s)$ and the following equality is obtained at the steady-state:

$$u_c = -|C(j\omega)| |P(j\omega)| K_{\text{DB}}(K_{\text{DBI}}(a) |A(j\omega)| a) K_{\text{DBI}}(a) \times |A(j\omega)| a \sin(\omega t + \phi_A(j\omega) + \phi_P(j\omega) + \phi_C(j\omega)) \quad (9)$$

where $\phi_C(j\omega)$ is the phase angle of $C(j\omega)$. When a limit cycle exists, $u_c(t)$ in Eq. (9) is equal to or approximately equal to $a \sin(\omega t)$ as assumed in the above, which results in the following necessary conditions for the existence of a limit cycle:

$$K_{\text{DBI}}(a) K_{\text{DB}} |C(j\omega)| |A(j\omega)| |P(j\omega)| = 1$$

$$\phi_C(j\omega) + \phi_A(j\omega) + \phi_P(j\omega) = \pi + 2k\pi, \quad k = 0, 1, 2, \dots \quad (10)$$

or equivalently in a complex form

$$K_{\text{DBI}}(a) K_{\text{DB}} C(j\omega) A(j\omega) P(j\omega) + 1 = 0 \quad (11)$$

It is obvious, if K_{DB} and K_{DBI} are constants, i.e., the DB and DBI blocks are linear systems, Eq. (11) is nothing but the conventional closed-loop characteristic equation with $s=j\omega$, i.e., a pair of complex closed-loop poles at $\pm j\omega$, a necessary condition for the closed-loop system to exhibit a steady-state sinusoidal type periodic solution of frequency ω .

If the closed-loop system does have a limit cycle of fundamental frequency ω , with the describing function approximation to the nonlinear elements, the fundamental frequency ω and the magnitude of the steady-state limit cycle a should satisfy Eq. (11). Thus, given the plant and actuator dynamics, $P(s)$ and $A(s)$, Eq. (11) can be used to provide a systematic way to analyze how the magnitude and frequency of the limit cycle, if it does exist, depend on the parameters of the controller $C(s)$, from which a well-informed decision could be made to select the specific controller parameters to optimize control performance in implementation.

Though the presented describing function analysis is based on linear time-invariant (LTI) system dynamics and controllers, it is not limited to linear systems with linear controllers. As mentioned in the above, the deadband effect mainly shows up during the regulation period around the target equilibrium point when the input signal to the deadband is small. Thus, for nonlinear dynamic systems with nonlinear controls, the closed-loop system's behavior during the transient period when the signals are large can be analyzed without considering the deadband effect. During the

steady-state period when the system is very close to the target equilibrium point, it is reasonable to linearize the nonlinear system dynamics and nonlinear controllers around the target equilibrium point and to apply the analysis presented in this section to check the local behavior of the linearized system, as done in Sec. 3.

3 Performance Optimization of Electrohydraulic Systems

3.1 Dynamic Model. In this section, the swing motion control of the hydraulic arm detailed in Ref. [8] is used as a case study. The system consists of a closed-center PDC valve, a single-rod double-acting hydraulic cylinder, and a mechanical linkage to convert linear cylinder motion into rotary joint motion. The cylinder and mechanical system dynamics are considered as the system dynamics to be controlled, while the valve dynamics is the actuator dynamics.

Off-line system identification on the valve-spool displacement frequency response reveals that the valve dynamics have a bandwidth around 8.5 Hz. Furthermore, below 10 Hz the dynamics can be very well approximated by the following second-order LTI dynamic model:

$$A(s) = \frac{X_{sp}(s)}{U(s)} = \frac{0.9 \times 51.5^2}{s^2 + 2 \times 0.66 \times 51.5s + 51.5^2} \quad (12)$$

where x_{sp} is the spool displacement normalized to have the same unit as the input signal, and u is the normalized control input to the valve ranging from -10 V to $+10$ V. Due to the deadband x_{DB} , the valve would not open until the spool displacement x_{sp} is larger than x_{DB} . Therefore, a virtual spool displacement or the actual valve opening can be defined as

$$x_{vr} = \begin{cases} x_{sp} - x_{DB}, & x_{sp} > x_{DB} \\ 0, & -x_{DB} \leq x_{sp} \leq x_{DB} \\ x_{sp} + x_{DB}, & x_{sp} < -x_{DB} \end{cases} \quad (13)$$

All signals in the above equations, x_{sp} , x_{vr} , and x_{DB} , are normalized to have the same unit as the input signal. The value of the deadband x_{DB} is equivalent to 1.0 V.

Neglecting cylinder flow leakages, the hydraulic cylinder equations can be written as [10]

$$\begin{aligned} \frac{V_1(x_L)}{\beta_e} \dot{P}_1 &= -A_1 \dot{x}_L + Q_1 = -A_1 \frac{\partial x_L}{\partial q} \dot{q} + Q_1 \\ \frac{V_2(x_L)}{\beta_e} \dot{P}_2 &= A_2 \dot{x}_L - Q_2 = A_2 \frac{\partial x_L}{\partial q} \dot{q} - Q_2 \end{aligned} \quad (14)$$

where A_1 and A_2 are the cylinder ram areas in the head-end and the rod-end, respectively, $V_1(x_L) = V_{h1} + A_1 x_L$ and $V_2(x_L) = V_{h2} - A_2 x_L$ are the total cylinder volumes of the head- and rod-ends including connecting hose volumes, respectively, V_{h1} and V_{h2} are the initial control volumes when $x_L = 0$, β_e is the effective bulk modulus, $\partial x_L / \partial q$ describes the relationship between the robot arm joint angle q to the cylinder rod displacement x_L and is a function of joint angle q , and Q_1 and Q_2 are the supply and return flows, respectively, which satisfy the orifice equation

$$\begin{aligned} Q_1 &= k_{q1} x_{vr} \sqrt{|\Delta P_1|} \\ Q_2 &= k_{q2} x_{vr} \sqrt{|\Delta P_2|} \end{aligned} \quad (15)$$

where k_{q1} and k_{q2} are orifice flow coefficients, which can be obtained through off-line system identification, x_{vr} is the actual valve opening, and ΔP_1 and ΔP_2 are the pressure drops across the valve.

The nominal swing motion dynamics, neglecting external disturbances, can be described by [1,11]

Table 1 System coefficients and parameters

Coefficient	Value	Description
β_e	4.24×10^8	Effective bulk modulus
k_{q1}	3.59×10^{-8}	Orifice flow coefficient
k_{q2}	3.72×10^{-8}	Orifice flow coefficient
A_1	0.00203	Cylinder ram area
A_2	0.00106	Cylinder ram area

$$J \cdot \ddot{q} = \frac{\partial x_L}{\partial q} (P_1 A_1 - P_2 A_2) - D_f \cdot \dot{q} \quad (16)$$

where q represents the swing joint angle, J is the moment of inertia of the swing motion, x_L represents the swing hydraulic cylinder displacement, P_1 and P_2 are the head- and rod-end pressures of the cylinder, respectively, A_1 and A_2 are the head- and rod-end ram areas of the cylinder, respectively, and D_f is the damping and viscous friction coefficient. The specific form of J is given in Ref. [1].

3.2 Nonlinear Controller Design. Advanced nonlinear controllers, such as the adaptive robust control (ARC) technique developed by Yao and co-worker in Refs. [12,13], are able to deal with both uncertain nonlinearities and parametric uncertainties effectively. For simplicity, the following analysis is done based on nominal nonlinear plant dynamics only, as the effect of external disturbances and various uncertainties can be effectively attenuated by the advanced nonlinear control techniques, such as ARC in Refs. [12,13].

As described in Secs. 1 and 2, the controller design will be done by neglecting the actuator or valve dynamics and using the direct deadband inverse to compensate for the sandwiched deadband. Thus, in the following, a nonlinear controller will be designed based on the plant (i.e., the cylinder and swing motion dynamics) only. The nonlinear controller design follows the standard backstepping design technique [14]. The objective is to let the system output q track a desired trajectory q_d as close as possible. Defining a set of variables $x_1 = q$, $x_2 = \dot{q}$, and $x_3 = P_1 A_1 - P_2 A_2$, as well as the fictitious control input $Q_L = (A_1 / V_1) Q_1 + (A_2 / V_2) Q_2$, the plant dynamics including swing motion dynamics and essential cylinder dynamics can be rewritten in a compact form as

$$\begin{aligned} \dot{x}_1 &= x_2 \\ \dot{x}_2 &= \frac{1}{J} \left[\frac{\partial x_L}{\partial q} x_3 - D_f x_2 \right] \\ \dot{x}_3 &= \beta_e \left[Q_L - \left(\frac{A_1^2}{V_1} + \frac{A_2^2}{V_2} \right) \frac{\partial x_L}{\partial q} x_2 \right] \end{aligned} \quad (17)$$

and the fictitious control input Q_L is related to x_{vr} by

$$Q_L = k_{Qeq} x_{vr} \quad (18)$$

where $k_{Qeq} = ((A_1 / V_1) k_{q1} \sqrt{|\Delta P_1|} + (A_2 / V_2) k_{q2} \sqrt{|\Delta P_2|})$. Table 1 shows the coefficients and parameters of the system under investigation.

Step 1. Define the tracking error as $z_1 = x_1 - x_{1d}$, where $x_{1d} = q_d$ is the desired trajectory. Then

$$\dot{z}_1 = \dot{x}_1 - \dot{x}_{1d} = x_2 - \dot{x}_{1d} \quad (19)$$

Since the system state x_2 is the mathematical input of the dynamic equation (19), it is usually called a virtual input to Eq. (19). The objective in this step is by adjusting x_2 to make the output z_1 converge to zero as quickly as possible. The mathematical description of the desired x_2 , referred as the virtual control law α_1 , can be designed as

$$\alpha_1 = \dot{x}_{1d} - k_1 z_1 \quad (20)$$

Step 2. Define z_2 be the discrepancy between the virtual control law α_1 and the system state x_2 as $z_2 = x_2 - \alpha_1$. Differentiating z_2 while noting Eq. (17), one can get

$$\dot{z}_2 = \frac{1}{J} \left(\frac{\partial x_L}{\partial q} x_3 - D_f x_2 \right) - \dot{\alpha}_1 \quad (21)$$

Considering x_3 is the input (21), a virtual control law α_2 can be designed as

$$\alpha_2 = \frac{1}{\frac{\partial x_L}{\partial q}} \left[(D_f x_2 + J \dot{\alpha}_1 - J(k_2 z_2 + z_1)) \right] \quad (22)$$

Step 3. Let $z_3 = x_3 - \alpha_2$ denote the input discrepancy. Differentiating z_3 while noting Eq. (17), one can get

$$\dot{z}_3 = \dot{x}_3 - \dot{\alpha}_2 = \beta_e \left[Q_L - \left(\frac{A_1^2}{V_1} + \frac{A_2^2}{V_2} \right) \frac{\partial x_L}{\partial q} x_2 \right] - \dot{\alpha}_2 \quad (23)$$

In viewing Eq. (23), Q_L is the control input and a control law Q_{Ld} can be synthesized as

$$Q_{Ld} = \left(\frac{A_1^2}{V_1} + \frac{A_2^2}{V_2} \right) \frac{\partial x_L}{\partial q} x_2 + \frac{1}{\beta_e} \dot{\alpha}_2 - \frac{1}{\beta_e} \left(k_3 z_3 + \frac{1}{J} \frac{\partial x_L}{\partial q} z_2 \right) \quad (24)$$

The k_i , $i=1,2,3$ in Eqs. (20) and (24) are all positive gains chosen to make the closed-loop system stable and have the desired bandwidth high enough to attenuate model uncertainties and reject disturbances reasonably well.

Defining $V(t) = \frac{1}{2}(z_1^2 + z_2^2 + z_3^2)$ and differentiating $V(t)$,

$$\begin{aligned} \dot{V} &= z_1(z_2 + \alpha_1 - x_{1d}) + z_2 \left\{ \frac{1}{J} \left[\frac{\partial x_L}{\partial q} (z_3 + \alpha_2) - D_f x_2 \right] - \dot{\alpha}_1 \right\} \\ &\quad + z_3 \left\{ \beta_e \left[Q_{Ld} - \left(\frac{A_1^2}{V_1} + \frac{A_2^2}{V_2} \right) \frac{\partial x_L}{\partial q} x_2 \right] - \dot{\alpha}_2 \right\} \\ &= -k_1 z_1^2 - k_2 z_2^2 - k_3 z_3^2 \leq -2 \min\{k_1, k_2, k_3\} V \end{aligned} \quad (25)$$

Therefore, the closed-loop system without considering the dead-band is exponentially stable with the convergence rate for $V(t)$ no less than two times of the minimum of k_1 , k_2 , and k_3 .

Step 4. The desired actual valve opening to deliver the flow control law (24) can be backed out from Eq. (18) as

$$x_{vrd} = \frac{1}{k_{Qeq}} Q_{Ld} \quad (26)$$

3.3 Closed-Loop Characterization. As commented at the end of Sec. 2, the analysis of this paper is only used to check the local behavior of the closed-loop nonlinear dynamics around the target equilibrium points. As such, linearize the plant dynamics (17) at the target equilibrium point $x_{eq} = [0, 0, 0]^T$,

$$\dot{x} = Ax + Bx_{vr} \quad (27)$$

where

$$A = \begin{pmatrix} 0 & 1 & 0 \\ 0 & \frac{D_f}{J} & \frac{1}{J} \frac{\partial x_L}{\partial q} \\ 0 & -\beta_e \left(\frac{A_1^2}{V_1} + \frac{A_2^2}{V_2} \right) \frac{\partial x_L}{\partial q} & 0 \end{pmatrix}_{x_{eq}} \quad (28)$$

$$B = [0 \ 0 \ k_{Qeq} \beta_e]^T|_{x_{eq}}$$

Similarly linearizing the nonlinear controller given by Eqs. (24) and (26) around the equilibrium point leads to

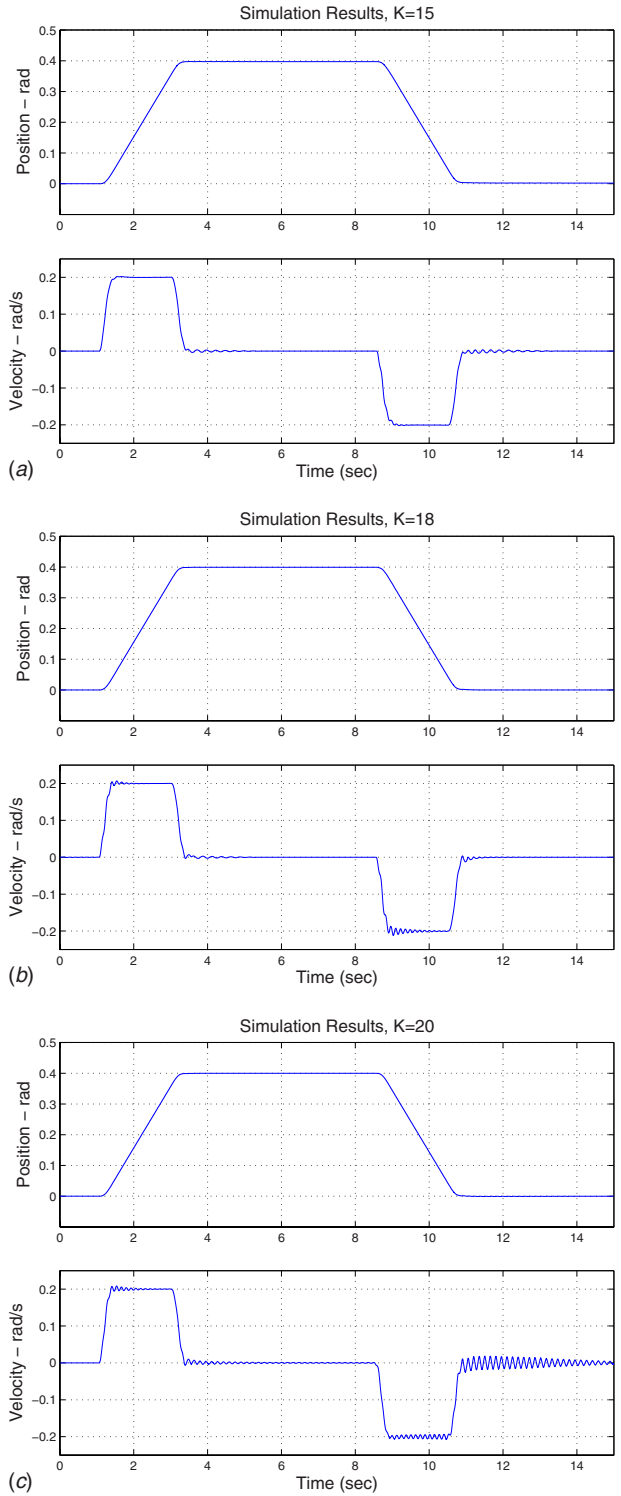


Fig. 5 Simulation results for different K value

$$x_{vrd} = -Cx, \quad C = \frac{1}{k_{Qeq}} [c_{k1}, c_{k2}, c_{k3}]^T|_{x_{eq}} \quad (29)$$

where $c_{k1} = 1/\beta_e \{ (\partial q / \partial x_L) J (k_1 k_2 k_3 + k_3) + (1/J) (\partial x_L / \partial q) k_1 \}$, $c_{k2} = -(A_1^2/V_1 + A_2^2/V_2) \partial x_L / \partial q + 1/\beta_e [(-\partial q / \partial x_L) D_f (k_1 + k_2 + k_3 - D_f/J) + J(k_1 k_2 + k_2 k_3 + k_3 k_1 + 1)] + (1/J) (\partial x_L / \partial q)$, and $c_{k3} = 1/\beta_e (-D_f/J)$

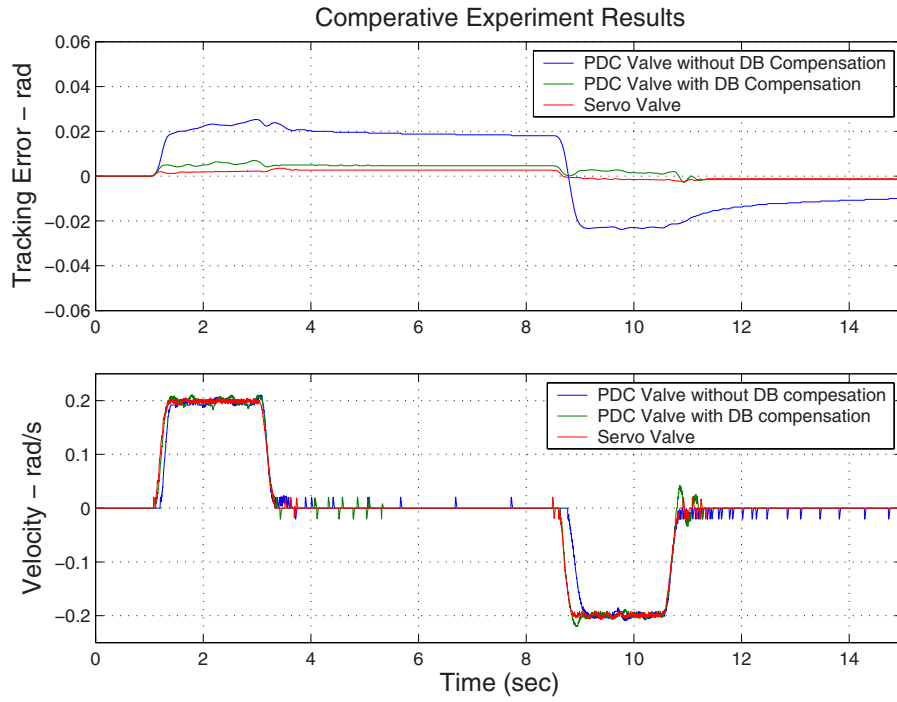


Fig. 6 Comparative experiment results

$+k_1+k_2+k_3$). For simplicity, one can assume $k_1=k_2=k_3=k>0$.² From Eqs. (27) and (29), the overall dynamics from the actual valve opening x_{vr} to the desired valve control input x_{vrd} of the linearized plant dynamics and the controller can be described by the following transfer function $-P(s)$:

$$P(s) = \frac{-X_{vrd}(s)}{X_{vr}(s)} = C(sI - A)^{-1}B$$

$$= \frac{(3k - 0.4)s^2 + (3k^2 - 593)s + (k^3 + k)}{s(s^2 + 0.4s + 594)} \quad (30)$$

Neglecting the actuator dynamics $A(s)$ and assuming the dead-band is perfectly canceled by its inverse function, $P(s)$ is then the open-loop transfer function of the system that includes the plant as well as the controller dynamics, and the resulting closed-loop transfer function would be

$$\frac{P(s)}{1 + P(s)} = \frac{(3k - 0.4)s^2 + (3k^2 - 593)s + (k^3 + k)}{s^3 + 3ks^2 + (3k^2 + 1)s + (k^3 + k)} \quad (31)$$

which is stable and has three closed-loop poles around $-k$ as predicted in the previous nonlinear design.

In reality, when the deadband is not perfectly canceled, the actual closed-loop would be in the general sandwiched deadband system described in Fig. 1 with $P(s)$ here represents the lumped linearized plant and controller dynamics given by Eq. (31). Applying the previous describing function analysis to this system, one obtains the following necessary condition for the existence of a limit cycle of period ω and amplitude of a as

$$K_{DBI}(a)K_{DB}(K_{DBI}(a)|A(j\omega)|a)A(j\omega)P(j\omega) + 1 = 0 \quad (32)$$

Note that the above equation only depends on the controller gain k . If k is already fixed, one can easily check whether a limit cycle would exist by solving Eq. (32). On the other hand, one can use

²In backstepping design, loosely speaking, each k_i represents the converging rate of the closed-loop dynamics in the corresponding step. By making them all have the same value, one can make various loops have the same converging rate. This is different from the conventional design where the inner loop is required to have much higher converging rate or bandwidth than the outer loop.

the result to optimize the controller design, i.e., choose the largest gain k , which is good in terms of faster closed-loop response and disturbance attenuation and thus leads to a less conservative controller, without causing the appearance of residual limit cycles, as illustrated below.

While analytically solving Eq. (32) may be difficult, numerically searching the solution is not difficult at all. Specifically, noting that K_{DBI} and K_{DB} are non-negative real numbers, the phase condition of Eq. (32) becomes

$$\angle A(j\omega) + \angle P(j\omega) = 180 \text{ deg} \quad (33)$$

which depends on the controller gain k and ω only. Thus, given k , it is easy to determine if there exists an ω that satisfies Eq. (33). The magnitude condition of Eq. (32) can then be used to determine if there exists an amplitude a as well. It is found through a searching program written in MATLAB that when k is increased to 17.5, there exists a solution of a and ω to Eq. (32). The limit cycle frequency ω for $k=17.5$ is about 47 rad/s or 7.5 Hz.

4 Simulations and Experiments

Simulations were done to check whether the proposed technique can predict the appearance of limit cycles accurately. The primary concern is whether the limit cycle happens around the predicted threshold of the controller gain k in avoiding limit cycles rather than the limit cycle frequency or magnitude. Three controllers with gains around the predicted threshold gain of 17.5 at the end of Sec. 3 and other values are simulated. The simulations were based on a more comprehensive model of the physical system than the controller design model used in Sec. 3.

When the system is moving at high speed, the valve is widely open and the overlapped spool or deadband would have a little effect on the system performance. The overlapped spool or deadband has a significant effect when the system comes to a stop; the spool may need to travel back and forward to make fine adjustment to satisfy the desired positioning accuracy requirement. Therefore, instead of high speed motion profile, a slow motion with a large portion being in the position regulation period is used

to best illustrate the deadband effect; the reference trajectory was a point-to-point smooth trajectory with a total movement angle of 0.4 rad and a maximum speed of 0.2 rad/s.

The first controller has the gain $k=15$, less than the predicted threshold gain. The second controller's gain $k=18$ is almost equal to the predicted threshold, and the third one's gain is $k=20$. Simulation results in Fig. 5 show that severe oscillation happens when the gain k is increased to 20, which is very close to the predicted threshold. The small discrepancy between the gain and predicted threshold could easily be due to the approximation nature of describing function method. The damped oscillation instead of sustained limit cycle is because the comprehensive simulation model used in simulation does include some damping effects, such as nonlinear Coulomb friction, which are neglected in the controller design model.

Experiments were also done to show if the controller gains can be chosen less conservatively with the proposed method. Bear in mind that the experimental setup is a large three-link hydraulic robot arm with neglected vibration modes that are not so high. A limit cycle or lightly damped oscillation could excite the vibration modes and cause instability. It is too dangerous to let such a large system become unstable. So no attempt is made to find the least conservative gain by increasing the gain until the system becomes unstable. Instead, a qualitative comparison was done to determine the upper and lower performance limits of a controller with sandwiched deadband. Specifically, the lower performance limit is defined as the performance of the above controller and PDC valve without deadband compensation. The upper performance limit is obtained by using the same controller but with a critically center servovalve (i.e., no physical deadband) having similar flow capacity as the above PDC valve and faster dynamic response. Comparative experimental results in Fig. 6 reveal that the performance of the controller with PDC valve and deadband compensation is very close to the upper performance limit obtained by the servovalve. This indirectly demonstrates the less conservative tuning of the proposed method in implementation.

5 Conclusions

Direct deadband compensation without taking the actuator dynamics into account has been the major design strategy for systems with sandwiched deadband so far due to the simplicity and easy implementation of the resulting controller. However, the controller is normally tuned very conservatively based on the empirical rule that the closed-loop bandwidth has to be much lower than that of the actuator dynamics to safely neglect the actuator dynamics in the design. This paper proposed a describing function based technique to systematically analyze and characterize the closed-loop performance of controllers with direct deadband compensa-

tion for systems with sandwiched deadband. Such an analysis gives the designer useful insights such as if limit cycles could happen when the controller parameters are tuned aggressively. The results thus help relax the conservativeness of the direct deadband compensation design when optimizing the achievable performance in implementation. Application of the proposed method to the control of a highly nonlinear electrohydraulic system shows accurate prediction of limit cycles in simulation and much improved closed-loop performance in experiments.

Acknowledgment

The work is supported in part by the US National Science Foundation (Grant No. CMS-0600516) and in part by the National Natural Science Foundation of China (NSFC) under the Joint Research Fund for Overseas Chinese Young Scholars (Grant No. 50528505).

References

- [1] Bu, F., and Yao, B., 2000, "Nonlinear Adaptive Robust Control of Hydraulic Actuators Regulated by Proportional Directional Control Valves With Deadband and Nonlinear Gain Coefficients," American Control Conference, Chicago, IL, pp. 4129–4133.
- [2] Tao, G., and Kokotovic, P. V., 1996, *Adaptive Control of Systems With Actuator and Sensor Nonlinearities*, Wiley, New York.
- [3] Taware, A., Tao, G., and Teolis, C., 2001, "An Adaptive Dead-Zone Inverse Controller for Systems With Sandwiched Dead-Zones," Proceedings of the American Control Conference, Arlington, VA, pp. 2456–2461.
- [4] Liu, S., and Yao, B., 2008, "Coordinate Control of Energy-Saving Programmable Valves," IEEE Trans. Control Syst. Technol., **16**(1), pp. 34–45.
- [5] Fortgang, J. D., George, L. E., and Book, W. J., 2002, "Practical Implementation of a Dead Zone Inverse on a Hydraulic Wrist," Proceedings of the ASME International Mechanical Engineering Congress and Exposition, New Orleans, LA, pp. 2002–39351.
- [6] Krylov, N., and Bogolyubov, N., 1947, *Introduction to Nonlinear Mechanics*, Princeton University Press, Princeton, NJ.
- [7] Gelb, A., and Velde, W. V., 1968, *Multiple-Input Describing Functions and Nonlinear System Design*, McGraw-Hill, New York.
- [8] Yao, B., Bu, F., Reedy, J., and Chiu, G.T.-C., 2000, "Adaptive Robust Control of Single-Rod Hydraulic Actuators: Theory and Experiments," IEEE/ASME Trans. Mechatron., **5**(1), pp. 79–91.
- [9] Khalil, H. K., 2002, *Nonlinear Systems*, 3rd ed., Prentice-Hall, Englewood Cliffs, NJ.
- [10] Merritt, H. E., 1967, *Hydraulic Control Systems*, Wiley, New York.
- [11] Liu, S., and Yao, B., 2002, "Energy-Saving Control of Single-Rod Hydraulic Cylinders With Programmable Valves and Improved Working Mode Selection," The SAE Transactions-Journal of Commercial Vehicles, SAE 2002-01-1343, pp. 51–61.
- [12] Yao, B., and Tomizuka, M., 1997, "Adaptive Robust Control of SISO Nonlinear Systems in a Semi-Strict Feedback Form," Automatica, **33**(5), pp. 893–900.
- [13] Yao, B., 1997, "High Performance Adaptive Robust Control of Nonlinear Systems: A General Framework and New Schemes," Proceedings of IEEE Conference on Decision and Control, San Diego, CA, pp. 2489–2494.
- [14] Krstic, M., Kanellakopoulos, I., and Kokotovic, P. V., 1995, *Nonlinear and Adaptive Control Design*, Wiley, New York.